



Constraints of $\Delta\mu/\mu$ based on H_2 observations in QSO spectra at high redshifts

M. Wendt¹ and P. Molaro²

¹ Institute of Physics and Astronomy, University Potsdam, 14476 Potsdam, Germany
e-mail: mwendt@astro.physik.uni-potsdam.de

² Istituto Nazionale di Astrofisica – Osservatorio Astronomico di Trieste, Via Tiepolo 11, I-34131 Trieste, Italy

Abstract. This report summarizes the latest results on the proton-to-electron mass ratio μ we obtained from H_2 observations at high redshift in the light of possible variations of fundamental physical constants. The focus lies on a better understanding of the general error budget that led to disputed measurements of $\Delta\mu/\mu$ in the past. Dedicated observation runs, and alternative approaches to improve accuracy provided results which are in reasonable good agreement with no variation and provide an upper limit of $|\Delta\mu/\mu| < 1 \times 10^{-5}$ for the redshift range of $2 < z < 3$.

Key words. Cosmology: observations – Quasars: absorption lines – Early universe.

1. Introduction

Our Standard Model contains numerous fundamental physical constants whose values cannot be predicted by theory and therefore need to be measured through experiments (Fritzsch 2009). These are mainly the masses of the elementary particles and the dimensionless coupling constants. The latter are assumed to be time-invariant although theoretical models which seek to unify the four forces of nature usually allow them to vary naturally on cosmological scales. The proton-to-electron mass ratio, $\mu = m_p/m_e = 1836.15267245(75)$ ¹ and the fine-structure constant $\alpha \equiv e^2/(4\pi\epsilon_0\hbar c) \approx 1/137$ are two specific constants that can be probed in the laboratory as well as in the distant and early Universe. Observations of ab-

sorption lines in the spectra of intervening systems towards distant quasars (QSO) have been subject of numerous studies.

The fine-structure constant is related to the electromagnetic force while μ is sensitive primarily to the quantum chromodynamic scale (see, i.e., Flambaum et al. 2004). The Λ_{QCD} scale is supposed to vary considerably faster than that of quantum electrodynamics Λ_{QED} . Consequently, the change in the proton-to-electron mass ratio, if any, is expected to be larger than that of the fine structure constant. Hence, μ is an ideal candidate to search for possible cosmological variations of the fundamental constants.

A measure of μ can for example be obtained by comparing relative frequencies of the electro-vibro-rotational lines of H_2 as first applied by Varshalovich & Levshakov (1993) after Thompson (1975) proposed the general ap-

Send offprint requests to: M. Wendt

¹ 2010 CODATA recommended value.

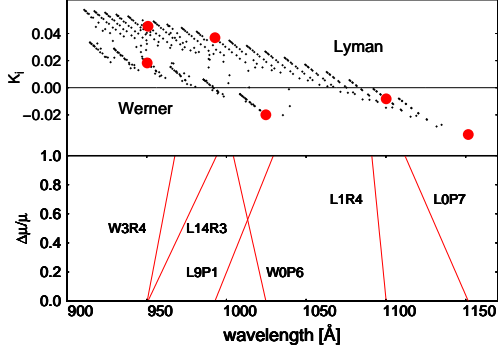


Fig. 1. The upper panel shows the sensitivity coefficients K_i of the Lyman and Werner transitions of H_2 against the restframe wavelength. Note, that the coefficients show different signs. The lower panel demonstrates the shifts of six selected transitions (marked with large red circles in the upper panel) with increasing $\Delta\mu/\mu$. For this illustration the range of $\Delta\mu/\mu$ is five orders of magnitude larger than the current constraints on $\Delta\mu/\mu$.

proach to utilize molecule transitions for μ -determination. The applied method uses the fact that the wavelengths of vibro-rotational lines of molecules depend on the reduced mass, M , of the molecule. Comparing electro-vibro-rotational lines with different sensitivity coefficients gives a measurement of μ .

The observed wavelength $\lambda_{\text{obs},i}$ of any given line in an absorption system at the redshift z differs from the local rest-frame wavelength $\lambda_{0,i}$ of the same line in the laboratory according to the relation

$$\lambda_{\text{obs},i} = \lambda_{0,i}(1+z) \left(1 + K_i \frac{\Delta\mu}{\mu} \right), \quad (1)$$

where K_i is the sensitivity coefficient of the i th component computed theoretically for the Lyman and Werner bands of the H_2 molecule (Meshkov et al. 2007; Ubachs et al. 2007). Figure 1 shows the sensitivity coefficients K_i for the Lyman and Werner transitions of H_2 in the upper panel. The coefficients are typically on the order of 10^{-2} . Since several coefficients differ in sign, some H_2 lines are shifted into opposite directions in case of a varying μ . The lower panel demonstrates this effect. The corresponding sensitivity coefficients are

marked as *filled red circles* in the upper panel. The expected shifts at the current level of the constraint on $\Delta\mu/\mu$ are on the order of a few 100 m s^{-1} or about $1/10^{\text{th}}$ of a pixel size.

Line positions are usually given as relative velocities with comparison to the redshift of a given absorption system defined by the redshift position of the lines with $K_i \approx 0$, then introducing the reduced redshift ζ_i :

$$\zeta_i \equiv \frac{z_i - z}{1+z} = K_i \frac{\Delta\mu}{\mu}. \quad (2)$$

The velocity shifts of the lines are linearly proportional to $\Delta\mu/\mu$ which can be measured through a regression analysis in the $\zeta_i - K_i$ plane. This approach is referred to as line-by-line analysis in contrast to the comprehensive fitting method (CFM) which will be discussed in section 4.

2. $\Delta\mu/\mu$ at the highest redshift

One of the latest results for $\Delta\mu/\mu$ is described in Wendt & Molaro (2012) and based on observations of QSO 0347-383. The damped Lyman- α system (DLA) at $z_{\text{abs}} = 3.025$ in its spectrum bears many absorption features of molecular hydrogen and represents the H_2 system with the highest redshift utilized for $\Delta\mu/\mu$ measurements. Numerous different results on $\Delta\mu/\mu$ in the redshift range of $2 < z_{\text{abs}} < 3$ led to the conclusion that the wavelength calibration had become the limiting factor in constraining $\Delta\mu/\mu$. Data of unprecedented quality in terms of resolution and calibration exposures was required. This and other aspects motivated the ESO Large Programme² and several data taken in advance to verify the spectrograph setup expected to provide the best results. The data of QSO 0347-383 were taken with the Ultraviolet and Visual Echelle Spectrograph (UVES) at the Very Large Telescope (VLT) on the nights of September 20-24 in 2009. The CCD pixels were not binned for these exposures for maximum resolution. A pixel size of $0.013 - 0.015 \text{ \AA}$, or 1.12 km s^{-1} at 4000 \AA along the dispersion direction was achieved. More details are given in Wendt & Molaro (2012).

² ESO telescope programme L185.A-0745

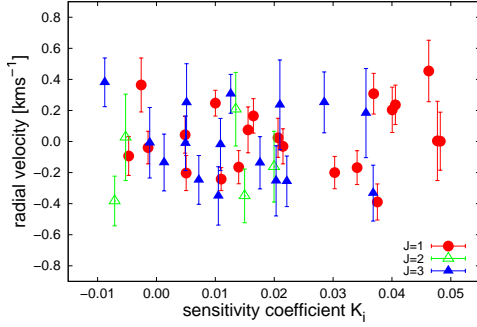


Fig. 2. Measured radial velocity vs. sensitivity for 42 H_2 lines observed in QSO 0347-383 in Wendt & Molaro (2012). Any correlation would indicate a change in μ . The different symbols correspond to the three observed rotational levels. The errorbars reflect the 1σ errors.

3. Results for QSO 0347-383

In Figure 2 the measured radial velocities of the 42 H_2 lines measured in QSO 0347 are plotted against the sensitivity coefficients K_i of the corresponding transition. Any correlation therein would indicate a variation of μ at $z_{\text{abs}} = 3.025$ with respect to laboratory values. The data give no hint towards variation of the proton-to-electron mass ratio in the course of cosmic time. The uncertainties in the line positions of the H_2 features due to the photon noise are estimated by the fitting algorithm. These are shown in the errorbars in Figure 2. The mean error in the line positioning is of 150 m s^{-1} . Even at first glance the given errorbars in Figure 2 appear to be too small to explain the observed scatter.

The scatter of lines with similar sensitivity coefficients K_i directly reflects the uncertainties in the line positions as it cannot be attributed to possible variations of μ since it is present for basically the same sensitivity parameter. The intrinsic scatter is of the order of 210 m s^{-1} and thus larger than the positioning error of the individual lines. That is also reflected by a reduced χ^2 of 2.7 for a weighted linear fit to the data (corresponding to $\Delta\mu/\mu = (1.8 \pm 8.2) \times 10^{-6}$ at $z_{\text{abs}} = 3.025$). The factual scatter of the data of the order of 210 m s^{-1} constitutes an absolute limit of pre-

cision. The above mentioned errors of the fitting procedure require an additional systematic component to explain the observed scatter:

$$\sigma_{\text{obs}} \sim \sqrt{\sigma_{\text{pos}}^2 + \sigma_{\text{sys}}^2}, \text{ with } \sigma_{\text{obs}} \approx 210 \text{ m s}^{-1},$$

$$\sigma_{\text{pos}} \approx 150 \text{ m s}^{-1}, \text{ and } \sigma_{\text{sys}} \approx 150 \text{ m s}^{-1}.$$

A direct linear fit to the unweighted data yields: $\Delta\mu/\mu = (4.2 \pm 7.7) \times 10^{-6}$. Bootstrap analysis is a robust approach to obtain an estimate of the underlying linear relation of the data in Figure 2 and estimate an error based on the true intrinsic scatter of the data. A gaussian fit to the bootstrap gives $\Delta\mu/\mu = (4.3 \pm 7.2) \times 10^{-6}$ and is in good agreement with the direct methods applied.

4. Challenges and risks

There are in principle two approaches to determine $\Delta\mu/\mu$ based on line centroid measurements of H_2 . For the analysis of QSO 0347-383 we applied a straight forward linear regression of the measured redshifts of individual H_2 absorption features and their corresponding sensitivity coefficients as plotted in Figure 1. This approach is referred to as line-by-line (LBL) analysis in contrast to the comprehensive fitting method (CFM).

The CFM fits all H_2 components along with additional H_1 lines and introduces an artificially applied $\Delta\mu/\mu$ as free parameter in the fit. The best matching $\Delta\mu/\mu$ is then derived via the resulting χ^2 curve. The CFM aims to achieve the lowest possible reduced χ^2 via additional velocity components. In this approach, the information of individual transitions is lost because merely the overall quality of the comprehensive model is judged.

The validity of the LBL or CFM approach depends mostly on the analyzed H_2 system. For example, the absorption in QSO 0347-383 (see Wendt & Molaro 2012) has the particular advantage of comprising merely a single velocity component, which renders observed transitions independent of each other and allow for this regression method. This was also tested in Rahmani et al. (2013) and King et al. (2008). For absorption systems with two or more closely and not properly resolved veloc-

ity components many systematic errors may influence distinct wavelength areas.

Weerdenburg et al. (2011), for example, increased the number of velocity components as long as the composite residuals of several selected absorption lines differed from flat noise. The uncertainties of the oscillator strengths f_i that are stated to be up to 50% in the same publication might, however, further affect the choice for additional velocity components. A similar effect can be traced back to the nature of the bright background quasar which in general is not a point-like source. In combination with the potentially small size of the absorbing clumps of H_2 , we may observe saturated absorption profiles with non negligible residual flux of quasar light not bypassing the H_2 cloud (see Ivanchik et al. 2010).

As pointed out by King et al. (2011), for multi-component structures with overlapping velocity components the errors in the line centroids are heavily correlated and a simple χ^2 regression is no longer valid. The same principle applies for co-added spectra with relative velocity shifts. The required re-binning of the contributing data sets introduces further auto-correlation of the individual 'pixels'.

Rahmani et al. (2013) discuss the assets and drawbacks of these two approaches in greater detail. The selection criteria for the number of fitted components are non-trivial and under debate. Prause & Reimers (2013) discuss the possibility of centroid position shifts due to incorrect line decompositions with regard to the variation of the finestructure constant α , which in principle is applicable to any high resolution absorption spectroscopy. Figure 3 shows a small extract of data from extensive simulations as an example of complex velocity and density structures that produce a multi-component absorption profile.

Additionally, thermal-pressure changes move in the cross dispersers in different ways, thus introducing relative shifts between the different spectral ranges in different exposures. There are no measurable temperature changes for the short exposures of the calibration lamps but during the much longer science exposures the temperature drifts generally by ≤ 0.2 K. The estimates for UVES are of 50 m s^{-1} for

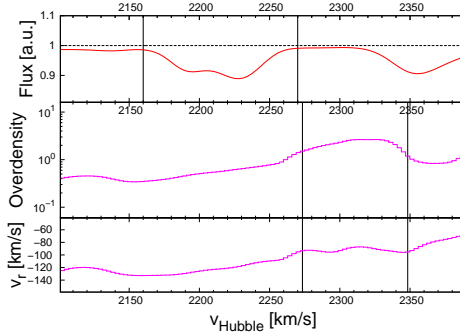


Fig. 3. Selected region from a simulated absorber as an example of a realistic density distribution (*center*) as well as macroscopic velocity fields (*bottom*) leading to a multi-component absorption feature (*top*). The corresponding interval is marked with vertical lines.

$\Delta T = 0.3$ K or a $\Delta P = 1$ mbar (Kaufer et al. 2004), thus assuring a radial velocity stability within $\sim 50 \text{ m s}^{-1}$.

The motion of Earth during observation smears out the line by $\pm 40 \text{ m s}^{-1}$, since the lineshape itself remains symmetric, this does not directly impact the centroid measurements but it will produce an absorption profile that is no longer strictly Gaussian (or Voigt) but rather slightly squared-shaped which further limits the quality of a line fit and must be considered for multi-component fits of high resolution spectra.

A stronger concern is the possibility of much larger distortions within the spectral orders which have been investigated at the Keck/HIRES spectrograph by comparing the ThAr wavelength scale with a second one established from I2-cell observations of a bright quasar by Griest et al. (2010). They find absolute offsets which can be as large as $500 - 1000 \text{ m s}^{-1}$ and an additional distortion of about 300 m s^{-1} within the individual orders.

This would introduce relative velocity shifts between different absorption features up to a magnitude the analysis with regard to $\Delta\mu/\mu$ is sensitive to. Whitmore et al. (2010) repeated the same test for UVES with similar results though the distortions fortunately show lower peak-to-peak velocity variations

of $\sim 200 \text{ m s}^{-1}$, and Wendt & Molaro (2012) detected an early indication of this effect directly in the measured positions of H_2 features as well as illustrated in Figure 4. Molaro & Centuri3n (2011) suggested to use the available solar lines atlas in combination with high resolution asteroid spectra taken close to the QSO observations to check UVES interorder distortions and published a revised solar atlas in Molaro & Monai (2012). Such asteroid spectra were used as absolute calibration to determine velocity drifts in their data via cross-correlation of individual wavelength intervals in Rahmani et al. (2013). They found distinct long range drifts of several 100 m s^{-1} within 1000 \AA . The origin of these drifts remains currently unknown but is under investigation and was considered by Bagdonaite et al. (2013) to contribute to their positive signal. Rahmani et al. (2013) found the drift to be constant over a certain epoch and applied suitable corrections. So far the drift, when present, in UVES spectra always showed the same trend at different magnitudes which could be an explanation for the reported tendency towards positive variation in μ (see next section).

5. Conclusions and outlook

Figure 5 shows the latest measurements of $\Delta\mu/\mu$ based on H_2 observations with UVES for 7 observed quasar spectra. The de-

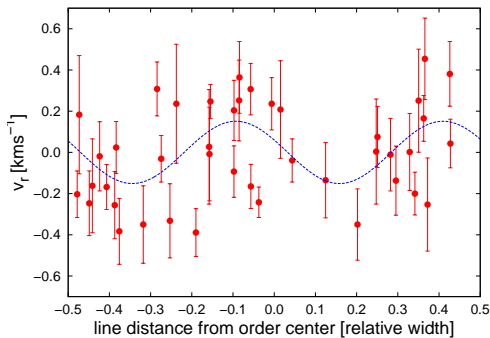


Fig. 4. All 42 lines with their radial velocity against their relative position within their order. A cosine fit with an amplitude of 151 m s^{-1} is shown in blue to indicate the possible intra-order distortion.

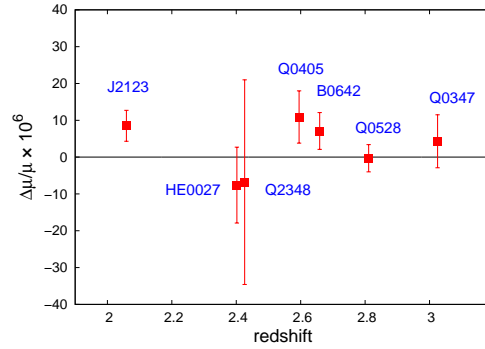


Fig. 5. Latest results for $\Delta\mu/\mu$ based on H_2 in seven different quasar sightlines observed with UVES: J2123-0050 (Weerdenburg et al. 2011), HE0027-1836 (Rahmani et al. 2013), Q2348-011 (Bagdonaite et al. 2012), Q0405-443 (King et al. 2008), B0642-5038 (Bagdonaite et al. 2013), Q0528-250 (King et al. 2011), Q0347-383 (Wendt & Molaro 2012). The given errorbars are the sum of statistical and systematic error (if both are given) under the assumption of gaussian distributed errors.

scribed measurements of QSO 0347-383 in Wendt & Molaro (2012) constitute the $\Delta\mu/\mu$ measurements via H_2 at the highest redshift to this day. The presented data of seven measurements yields a mean of $\Delta\mu/\mu = (3.7 \pm 3.5) \times 10^{-6}$ and is in good agreement with a non-varying proton-to-electron mass ratio. Such a generic mean value does not take into account any interpretation with regard to spatial or temporal variation and instead merely evaluates the competitive data available for $\Delta\mu/\mu$ based on H_2 -observations, which consequently are limited to the redshift range of $2 < z_{\text{abs}} < 3$ and the evidence these data provide for any non constant behavior of μ over redshift. This tight constraint already falsifies a vast number of proposed theoretical models for varying μ or α . Thompson et al. (2013) come to the conclusion that that “adherence to the measured invariance in μ is a very significant test of the validity of any proposed cosmology and any new physics it requires”.

The data from the ESO LP observations has the potential to set a new cornerstone in the assessment of variability of fundamental physical constants such as α or μ via measurements of H_2 at high redshifts. Observations

featuring instruments in the foreseeable future will provide further insights. Data taken with laser-comb calibrated spectrographs (such as CODEX or EXPRESSO) at large telescopes (E-ELT or VLT, respectively) implicate new methods of data analysis as well.

Acknowledgements. We are thankful to the organizers of the conference on “Varying fundamental constants and dynamical dark energy” in Sesto, Italy and express our gratitude to its attendants for numerous fruitful discussions. We also appreciate the helpful comments by Thorsten Tepper Garcia.

References

- Bagdonaite, J., Murphy, M. T., Kaper, L. and Ubachs, W. 2012, MNRAS, 421, 419
- Bagdonaite, J., Ubachs, W., Murphy, M. T. and Whitmore, J. B. 2013, ApJ submitted, arXiv:1308.1330v1
- Flambaum, V. V., Leinweber, D. B., Thomas, A. W. and Young, R. D. 2004, Phys. Rev. D, 69, 11506
- Fritzsche, H. 2009, Physics-Uspekhi, 52, 359
- Griest, K. et al. 2010, ApJ, 708, 158
- Ivanchik, A. et al. 2005, ApJ, 440, 45
- Ivanchik, A. V. et al. 2010, MNRAS, 404, 1583
- Kafer, A. et al. 2004, UVES User manual
- King, J. A., Webb, J. K., Murphy, M. T. and Carswell, R. F. 2008, Phys. Rev. Lett., 101
- King, J. A., Murphy, M. T., Ubachs, W. and Webb, J. K. 2011, MNRAS, 417, 3010
- Malec, A. L. et al. 2010, MNRAS, 403, 1541
- Meshkov, V. V., Stolyarov, A. V., Ivanchik, A. V., Varshalovich, D. A. 2006, JETPL, 83, 303
- Molaro, P., Centurión, M. 2011, A&A, 525, 74
- Molaro, P., Monai, S. 2012, A&A, 544, 125
- Murphy, M. T., Tzanavaris, P., Webb, J. K. and Lovis, C. 2007, MNRAS, 378, 221
- Murphy, M. T. et al. 2008, MNRAS, 384, 1053
- Prause, N., Reimers, D. 2013, A&A, 555, 88
- Rahmani, H. et al. 2013, MNRAS in press, arXiv:1307.5864v1
- Thompson, R. I. 1975, Astrophys. Lett., 16, 3
- Thompson, R. I. et al. 2009, ApJ, 703, 2
- Thompson, R. I., Bechtold, J., Black, J. H. and Martins, C. J. A. P. 2009, New A, 14, 379
- Thompson, R. I., Martins, C. J. A. P. and Vielzeuf, P. E. 2013, MNRAS, 428, 2232-2240
- Ubachs, W., Buning, R., Eikema, K. S. E. and Reinhold, E. 2007, J. Molec. Spec., 241, 155
- Varshalovich, D. A., Levshakov, S. A. 1993, JETP, 58, 231
- van Weerdenburg, F. et al. 2011, Phys. Rev. Lett., 106, 180802
- Wendt, M., Molaro, P. 2011, A&A, 526, 96
- Wendt, M., Molaro, P. 2012, A&A, 541, 69
- Whitmore, J. B., Murphy, M. T. and Griest, K. 2010, ApJ, 723, 89